Chem Soc Rev

RSC Publishing

TUTORIAL REVIEW

View Article Online
View Journal | View Issue

The use of *in situ* and *ex situ* techniques for the study of the formation mechanism of mesoporous silica formed with non-ionic triblock copolymers†

Cite this: *Chem. Soc. Rev.*, 2013, **42**, 3777

Tomas Kjellman* and Viveka Alfredsson

Since the discovery of the mesoporous silica material templated by ionic surfactants and the subsequent development of materials templated by non-ionic surfactants and polymers, for example SBA-15, there has been a continuous research effort towards understanding their formation. *In situ* methodologies, such as Small Angle X-ray Scattering (SAXS), Small Angle Neutron Scattering (SANS), spectroscopic techniques like NMR and EPR, and *ex situ* methodologies such as electron microscopy techniques (SEM, TEM and cryo-TEM) are powerful and important tools in the investigation of the mechanism by which these materials form. The need for a fundamental understanding of the systems is of academic concern and of great importance when developing materials for applications. In this tutorial review we aim to give the reader a comprehensive overview on the development of the field over the years and an introduction to the experimental *in situ* and *ex situ* techniques that have been used.

Received 31st July 2012

DOI: 10.1039/c2cs35298b

www.rsc.org/csr

Introduction

A remarkable discovery within the world of materials science in the past 20 years was the realisation of the possibility to synthesize ordered mesoporous materials (*i.e.* materials with pores in the range of 20–500 Å) with well-defined pore size. The first materials, MCM-41 (hexagonal *P6mm*), synthesized at Mobil,[1] and the equivalent material, synthesised with kanemite, a layered silicate, at Waseda University,[2] utilized cationic surfactants as structure directing agents. Mesoporous materials had been produced before but not with ordered pores with a narrow size distribution. Other ordered porous materials on the other hand, such as zeolites, has crystalline walls and pores in the micropore range. The combination of the interesting properties of the new mesoporous material sparked much interest within the community and an essentially new topic of research emerged. A few years after the synthesis of MCM-41, non-ionic surfactants were identified as possible structure directors,[3] and, by using the non-ionic triblock co-polymers with the trade name

Physical Chemistry, Lund University, P.O. Box 124, 221 00, Lund, Sweden. E-mail: tomas.kjellman@fkem1.lu.se

† Part of the mesoporous materials themed issue.

Tomas Kjellman

Tomas Kjellman was born in Lund, Sweden. He received his Master's degree in Chemistry from Lund University in 2009. The same year he started his current position as a PhD student at the division of Physical Chemistry, studying various aspects of SBA-15.

Viveka Alfredsson

Viveka Alfredsson, born in 1963, graduated with a Master of Science degree from Lund University in 1988 and received her PhD in Inorganic Chemistry from the same university in 1994. During 1995–1996 she was a Post Doctoral fellow at UMIST in Manchester, UK. After a short period in Industry she returned to Lund University in 1998. She was promoted to Professor in December 2011.

Pluronics, SBA-15[4,5] was synthesized by Zhao *et al.* at the University of Santa Barbara. Pluronic polymers consist of two poly(ethylene oxide) (PEO) blocks separated by a poly(propylene oxide) block (PPO). It was immediately realised that SBA-15 has thicker pore walls and larger pores than the structurally equivalent MCM-41. These properties gave SBA-15 a higher hydrothermal stability, an issue with MCM-41 and for instance its use in catalytic applications.

The basic synthesis protocol for SBA-15 is simple. A silica source is added to an acidic aqueous micellar solution of the non-ionic polymer at rather gentle temperatures, typically ranging from 20–80 °C. The synthesis mixture is kept for about 24 h at that temperature, then treated hydrothermally for 24 h at higher temperature. To obtain the porous material the structure director is subsequently removed either by calcination or extraction.

The original SBA-15 papers[4,5] also presented potential for tuning the material properties, thus opening up possibilities for a wider range of applications such as catalysis, drug delivery, adsorption, and separation. To make use of the potential for such diverse applications there is a need for a good characterisation and deeper understanding of the formation process, and the means of controlling it, of this material as well as other mesoporous silica materials that were synthesized in its wake.[6–8] For example, it was promptly shown that the first description of the structure of SBA-15 as a 2 dimensional arrangement of cylindrical mesopores was only partially correct. It turns out that there exist smaller, unordered channels (in the ultramicro- to small mesopore size range) connecting the main mesopores through the silica walls, effectively creating a 3 dimensional network.[9,10] These pores will be termed intrawall pores for the remainder of this review. Such a difference is of course of great importance regarding material properties.

This review will focus on the research that has been done up to now to elucidate the formation mechanism and the processes involved in going from a dilute micellar solution of non-ionic structure directors to the ordered mesoporous silica materials. In the first section a number of useful, and so far frequently used, experimental techniques are briefly described together with examples from the literature on how they have been applied to extract information on the synthesis process of mesoporous materials. The second section focuses on the formation process, (artificially) divided into three different periods, discussing what is known, inferred and suggested to occur based on the experimental findings throughout the literature. Finally some concluding remarks to summarize the discussion are made.

Techniques

In this section we aim to give an overview of the main experimental techniques that so far have been used in the study of the formation of mesoporous silica. We will give some very brief information about each technique but for a more comprehensive and detailed description textbooks and other specialised sources

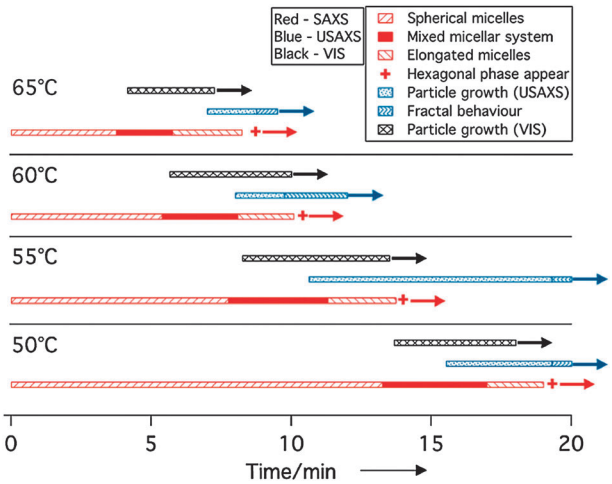

Fig. 1 The temporal evolution of a system during the synthesis of SBA-15 at different temperatures. Through the use of several complementary techniques, probing different length scales of components present in the reagent solution, a time line of formation events is proposed. Using several complementary techniques for investigating the formation is advantageous as the important formation events occur at different length scales. In addition both thermodynamic and kinetic effects are crucial to obtain a well-defined material and thus need to be considered. Reprinted with permission from ref. 11. Copyright 2009, American Chemical Society.

are recommended. Focus will instead be on the information that can be extracted for the particular purpose of this review, comprising the possibilities and limitations of the techniques. We will also provide examples from the current literature.

Elucidating the mechanism behind the formation of mesoporous silica is a complicated but important problem. Processes occur at length scales ranging from the Ångström to the micrometer scale and both thermodynamic and kinetic factors are of importance. A complete overview of the properties and aspects of formation thus requires the combination of several complementary techniques. An example showing results obtained from an investigation where several complementary techniques have been used is shown in Fig. 1. In the example shown X-ray scattering (SAXS and USAXS) and UV-vis, all measured *in situ*, were used to probe length scales from 1 nm to 1 μm over the time period enabling information to be gathered regarding micelles, larger objects (*i.e.* future particles), as well as the ordered materials.[11]

Scattering (including diffraction)

Scattering techniques are based on the uneven scattering over different angles of the incoming probing radiation caused by inhomogeneity in the investigated sample. For light scattering it is inhomogeneity in the diffraction index, for X-ray scattering it is inhomogeneity in the electron density of the sample, while for neutrons it is the atomic scattering length density (which depends on the nuclei of the elements that are present in the sample) that determines the variation of scattering. An important aspect of neutrons over other techniques is the possibility to "contrast match" certain parts, or more precisely components, of the sample with the solvent (often water) by varying the ratio of hydrogen (*i.e.* H_2O) and deuterium (*i.e.* D_2O). The difference in

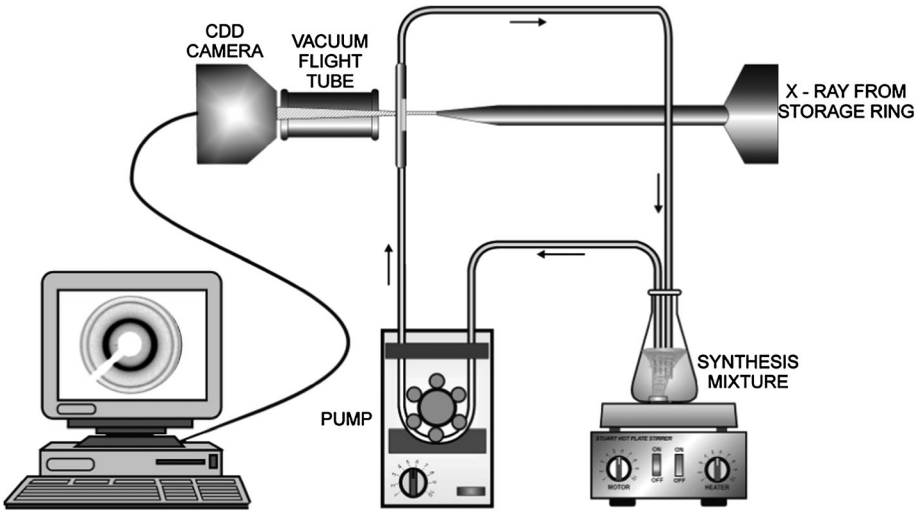

Fig. 2 The experimental set-up for *in situ* SAXS measurements used in ref. 15. The reagent solution is pumped, in a closed loop, from the stock solution, using a peristaltic pump, *via* the measuring capillary/cell, back to the stock solution. The temperature is held constant. Use of a 2D detector allows for probing of anisotropic behaviour. A synchrotron based X-ray source is typically needed to probe the rather fast formation dynamics. Reprinted with permission from ref. 15. Copyright 2005, American Chemical Society.

the so-called scattering length density of hydrogen and deuterium is very large and by varying the ratio, it is possible to match other components in the sample. The interesting parts of the structure in the sample can thus be highlighted while other parts are made "invisible". This approach has been used by several authors[12–14] to study the formation of *e.g.* SBA-15. However, neutrons require large-scale facilities such as ILL, ISIS and HFIR at Oak Ridge national laboratory, and while X-rays are more easily accessible and can give good data on in-house instruments, synchrotron radiation is more powerful due to the much higher intensity/flux and thus preferable for *in situ* studies. An example of an experimental set-up used for the *in situ* study of formation of SBA-15 is shown in Fig. 2.[15] The synthesis solution is pumped in a closed-loop from a flask, containing the largest volume of the reaction mixture, *via* the capillary placed in the beam and back to the flask. Hence all components, including precipitated material, are probed. The temperature of the reaction is kept constant.

Porous silica materials have been investigated in several studies using both *ex situ*,[16,17] *in situ* SAXS[11,12,15,18–26] (including Ultra Small Angle X-ray Scattering, USAXS[11]), *in situ* SANS,[13,27,28] and dynamic light scattering[26,29,30] providing information on the evolving systems, from the initial assembly of smaller molecules to the final structure and particle formation. The acquired scattering data are usually plotted as intensity *versus* scattering vector, $\boldsymbol{q}$. Typically, the diffuse micellar scattering, which is always observed at the onset of a synthesis, can be fitted to different models providing information about for example size, polydispersity and shape of the micelles. However, there is no guarantee that the model chosen is the only possible fit and supporting data from complementary methods is recommended. If Bragg peaks are present information about structural parameters can also be extracted. Note that the absence of Bragg peaks does not necessarily mean the absence of structure. This could be caused by for instance a high background scattering. An example of *in situ* SAXS data from the synthesis of SBA-15, taken from ref. 12, where the influence of four different acids was probed in the synthesis of SBA-15, is shown in Fig. 3. The intensity of the detected scattered radiation is increasing in the order of blue, green, yellow and red. Broad oscillations of lower intensity indicate the micellar scattering while sharp, high intensity peaks are the Bragg peaks of the ordered structure.

X-rays and neutrons can probe lengths from less than 1 nm to several hundreds of nm. Reaching large sizes, on the order of microns, with X-rays requires that one utilize an ultra small angle set-up, USAXS. However, the time-resolution in a USAXS investigation is restricted due to the experimental set-up. The possibility to readily perform *in situ* experiments on the relevant time scale makes scattering techniques of great use for investigating the dynamic aspects of many systems, not only porous ones.

NMR

Nuclear magnetic resonance spectroscopy can theoretically be used on any nuclei with an intrinsic magnetic moment and angular momentum, *i.e.* a nonzero spin. For the investigation of mesoporous materials ^{1}H,[31–33] ^{13}C,[33] ^{14}N,[34] ^{17}O,[34] ^{31}P[35] and ^{29}Si-NMR[17,31,33,34,36] have been used to study both the formation mechanism as well as other aspects such as presence of functional groups or assessing solid acid properties.[35] ^{29}Si-NMR is very often used to characterize the final material in terms of cross-linking of the silica structure since one can differentiate between Si-atoms covalently bonded, *via* an oxygen bridge, to one, two, three or four other Si-atoms.

The technique is non-invasive and very useful since the resonance frequency is dependent on the chemical environment of the investigated nucleus. Christiansen *et al.*[31] used different protocols for ^{29}Si-NMR to study the inorganic framework in silicate–surfactant mesophases while Flodström *et al.* used ^{1}H-NMR to follow the mobility of the methyl group of PEO–PPO–PEO block

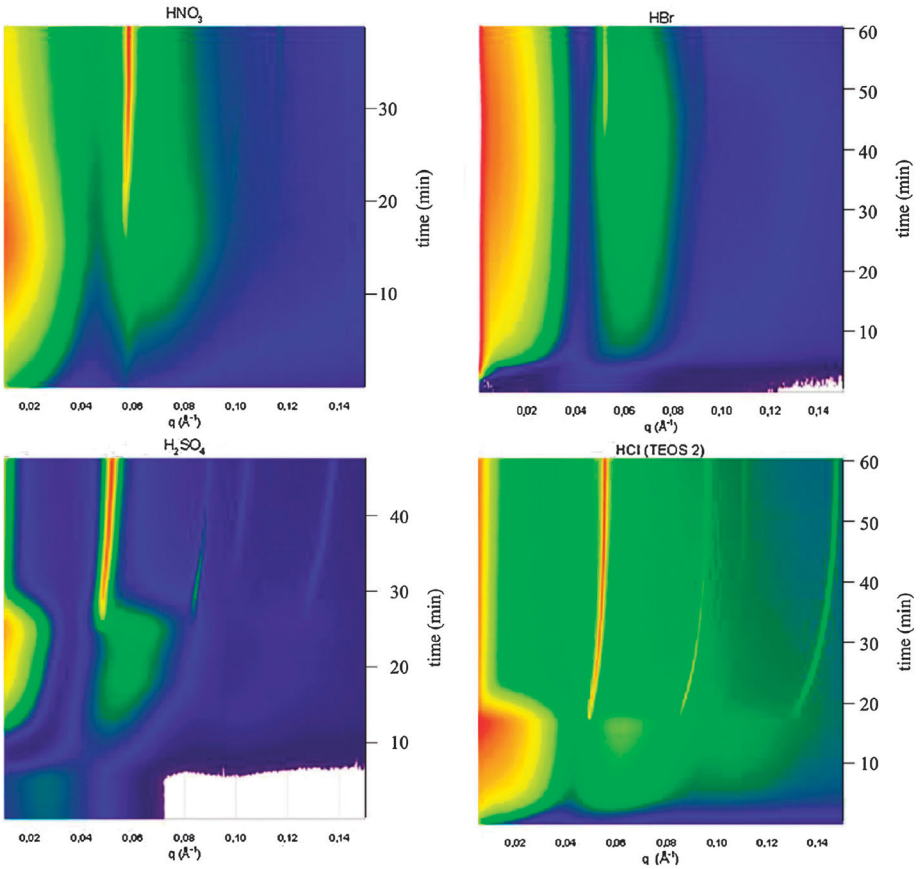

Fig. 3 *In situ* SAXS data from measurements of four syntheses using different acids (a) HNO_3, (b) HBr, (c) H_2SO_4 and (d) HCl. The scattered intensity is plotted upon time *vs.* the scattering vector, ***q***. The colours represent increasing intensity in the order of blue, green, yellow and red. The broad peak, at the beginning of the measurement (particularly clear in figure d) results from the micellar scattering while the sharp peaks are the Bragg peaks indicative of the *P6mm* structure. The Bragg peaks typically increase in intensity during the measurement and the change in position (increasing ***q***-spacing) is due to the unit-cell compression. Reprinted with permission from ref. 12. Copyright 2011, American Chemical Society.

copolymers in synthesis of both cubic and hexagonal mesoporous silica.[19,32]

Since only atoms with non-zero spin give rise to a signal in NMR, some elements, like for instance Si, the low abundance of the NMR sensitive isotope (^{29}Si) can cause the measurements to be lengthy and consequently of limited use for *in situ* studies. With a conventional NMR set-up the design of the instrument introduces limitation in for example stirring, which has recently been shown to be of importance for the material properties of SBA-15.[37]

EPR

Electron paramagnetic resonance spectroscopy is in many ways the equivalent of NMR, only electrons are probed instead of nuclei. Like the nucleus, a molecule can have non-zero spin, but it requires an unpaired electron, which makes the technique less straightforward. Silica formation using both cationic[38–41] and non-ionic[42–45] structure directors has been studied in detail with EPR. In these studies spin-probes, *i.e.* molecules that have a non-zero spin, are added to the synthesis solution. These probes were chosen so that they preferentially locate in the region of interest and thus provide information about the changes in the system from that specific region. In Fig. 4[43] a Pluronic micelle is schematically illustrated with the locations of a number of different spin-probes that have been used, marked by numbers (see Fig. 4). The use of a spin-probe

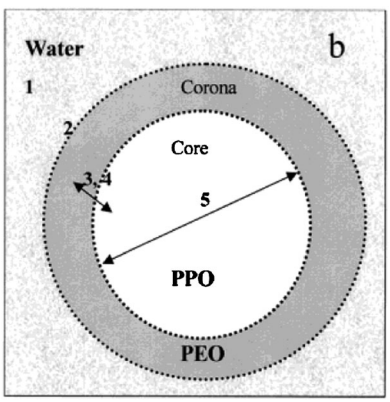

Fig. 4 Schematic representation of a Pluronic micelle in water, with a hydrophobic core and a hydrophilic corona consisting of PPO and PEO respectively. This is the normal representation but the interface between the two regions is of a more continuous nature. The different numbers represent regions where spin probes, used for EPR-spectroscopy measurements in ref. 43, preferentially locate. Adapted with permission from ref. 43. Copyright 2003, American Chemical Society.

requires additional effort, first by finding a suitable probe and then by verifying that the probe is located in the region of interest. Also, the introduction of another species into the system under study could possibly influence it. However, if the location of the spin-probe is well established and that its effect on the synthesis is negligible, EPR is a powerful tool for investigating time-dependent processes. Further the ability to probe different locations in the micelles by use of spin probes, as mentioned above, is naturally a great advantage of this technique.

Electron microscopy

There are two primary categories of electron microscopy; transmission and scanning electron microscopies (abbreviated TEM and SEM respectively).

In TEM, the sample is irradiated by electrons with high energy (hundreds of kV), passing through the thin sample to give an image with a contrast based on the electron density of the sample. If the sample contains ordered structures these can be observed either from a diffraction pattern or from the image directly. The ordered structure for mesoporous materials is on the nanometer length scale but TEM instruments as such are capable of providing atomistic resolution (albeit not for these types of atomically amorphous materials).

In SEM the energy of the electrons bombarding the sample is much lower (from less than 1 kV up to 20 kV), and the beam is scanned over the sample. The electrons, either being back-scattered or secondary electrons emitted from the sample, are probed by the detector, being located on the same side of the sample as the electron source. In general we can say that SEM provides topographic surface information down to the nanometer level as well as information on a much larger scale such as *e.g.* information on particle morphology and aggregation.

Both TEM and SEM are very powerful characterization techniques as they provide a direct image of the specimen. However, the sampled material is small compared to averaging techniques such as scattering and NMR. They are also limited to *ex situ* studies and, in conventional SEM and TEM, only solid samples can be investigated. This makes them less useful for the study of the formation mechanism of mesoporous silica since the formation is an ongoing process and the system is inherently a soft matter system (at the early stages of formation). Nevertheless, Flodström *et al.*[32] used TEM to study the formation of SBA-15 using an approach, previously used for the study of nascent particles of MCM-41,[46] by which a small volume of solution from an on-going synthesis was diluted and then quickly transferred to a copper grid used for viewing samples. If applicable, cryogenic techniques (*i.e.* rapidly freezing a sample, with a rate of more than 10^4 K s^{-1}, during synthesis to ''arrest'' the formation at a particular time) are preferable and have been used by several authors. The ''arrested'' state can then be visualised and by sampling the synthesis at several points in time, ''snapshots'' of the formation can be recorded. This was initially done by Regev in the synthesis of MCM-41.[47] Later on, for SBA-15, it was used by Ruthstein *et al.*[48] to study solution structures during the formation, and recently by Ruan *et al.*[49] to study initial stages of formation. SEM (both normal and cryo) has been used to study both SBA-15[49–51] and cubic KIT-6,[45] as well as structure transformations from hexagonal to bicontinuous cubic structure.[52]

Electron microscopy techniques, while powerful, suffer from limitations. There is always sample preparation required, and as such, always a risk of altering the sample. Further, as mentioned above, the sampled material is very limited and might not be representative. Care should be taken to explore several areas of the investigated sample. The sample may also be affected by the energy of the probing electron beam. TEM is very efficient for studying ordered structures, but unordered structures are much more difficult to visualise. SEM generally suffers from charging problems. For non-conducting materials such as silica, this problem is usually avoided by sputter coating the sample with a conducting material such as gold. But since SEM is inherently a surface technique, coating the material under study naturally comes with a loss of surface information. There are ways to study non-conductive materials with SEM, *e.g.* low voltage electrons,[53] but it requires rather high-end instruments.

Formation mechanism

The study of the formation mechanism of mesoporous silica materials can, with some simplification, be divided into three periods of interest based on different formation events. They typically follow in this order but can be more or less temporally overlapping and affected by the progression of the previous periods.

- The micellar period – this period comprises the initial formation stages, including the state of the micelles before the addition of a silica source and following the onset of the synthesis after the addition. Studies related to the immediate interaction and association of siliceous species with the polymer micelles are placed under this section. Different systems can be quantitatively different during these initial stages but there is a consensus on the qualitative aspects.
- The micellar-to-structured material period – the development from isolated micelles with some silica associated to the early manifestations of particles and the occurrence and evolution of ordered structure are the most important events in this period. As we shall see there are different views on the progression of the systems here and the understanding is still not definite.
- The particle development period – we are in this period including data that describe mostly how the size, morphology and stability of the forming particles as well as their aggregation behaviour are developed.[49,51,54–56]

The division is as mentioned an artificial one, done in the interest of simplifying the process sufficiently to give an overview on which issues that have been addressed, which issues remain and the techniques that are appropriate to use for different investigations. The time scales for these periods vary depending on synthesis conditions, but in general the micellar period lasts for less than 30 min while the other periods can last substantially longer.

One could add a fourth period as well which would be focused on the post-synthesis events (*i.e.* hydrothermal treatment and calcination/extraction) but since this review is focused on the

formation process this will be mentioned only when results are interpreted as a consequence of the formation mechanism.

The micellar period

In a standard preparation, before the initiation of the synthesis, the structure directing agent is dissolved in aqueous media to give a dilute micellar solution. Such systems have been extensively studied for many years by polymer- as well as surface and colloid-chemists. The interested reader can read about molecular forces and interactions in such systems in textbooks on the subject.

The most common Pluronic polymer used to synthesize SBA-15 is Pluronic P123 (EO_{20}–PO_{70}–EO_{20}),[5,12,15,27,42,43,48,50,51,57–59] though others can be used as well.[5,11,22,43,49,54] The starting concentration of the polymer is usually about 2.5 wt%, which is well above the critical micellization concentration (CMC) at temperatures above room temperature. Pluronic micelles are generally spherical with aggregation number of around 100 under normal synthesis conditions[57] and have a core consisting of mainly PPO and typically some PEO, with a low level of hydration. The corona on the other hand, composed of the main part of the PEO segments, is extensively hydrated. Pluronic molecules have so-called reversed solubility, *i.e.* decreasing solubility with increasing temperature, suggested to be caused by a less favourable conformation of the ethyleneoxide moieties at high temperatures, reducing the level of hydrogen bonding.[60] At higher temperatures the aggregation number will typically increase but the size of the micelles remains approximately constant due to dehydration.[61]

The effect of salt on Pluronics is intriguing and tends to follow the well-known Hofmeister-series where different ions, in particular anions, have different influence. In a calorimetry study on the effects of salts on Pluronic L64 (EO_{13}–PO_{30}–EO_{13}), chloride and bromide were found to decrease both the critical micellization temperature (CMT) and the cloud point (CP). Iodide was found to increase the CP but decrease the CMT while SCN^- and urea were found to increase both the CMT and the CP.[62] While the literature on PEO and PPO block co-polymers is extensive, it is rarely with the expressed purpose of increasing the understanding of mesoporous silica formation. Manet *et al.* however have performed extensive SANS and SAXS studies on both evolving SBA-15 systems[12] as well as the pure polymer system under the same conditions.[57] The polymer (Pluronic P123) micelles in aqueous solution are found to be well described by a core–shell spherical model (see Fig. 5) with a hydrophobic core composed of PPO and under some conditions including more less of the PEO-chains. The corona is always, under the conditions used by Manet *et al.*,[57] composed of PEO with hydration levels of 80–90% while PEO in the core has a hydration level of only 20%. The authors discuss that the sharp "borders" in the core–shell model is a simplification; a more realistic transition would be continuous. The effect of different anions is investigated as well by using different mineral acids to achieve concentrations similar to those commonly used in the synthesis of SBA-15. The effects of the anions follow the Hofmeister series as expected, with "salting-in" ions (Br^- and NO_3^-) enriching in the micelles. Interestingly, no difference in

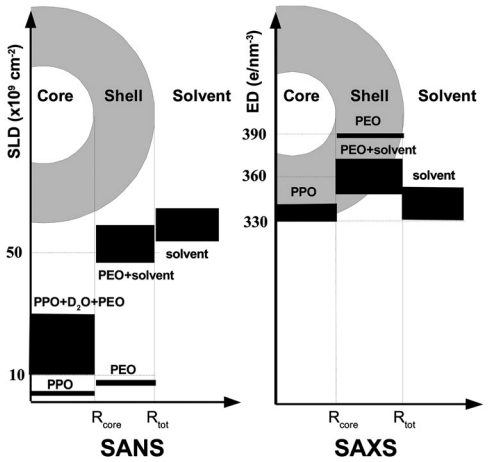

Fig. 5 The core–shell density model for SANS and SAXS respectively, used in ref. 57 is shown. The strength of scattering as a function of radius is plotted. In SANS the scattering length density (SLD) dictates the strength of scattering whereas in SAXS it is the electron density. SANS has the advantage that scattering can be tuned by using different contrasts (typically by varying the solvent) however the obtainable time resolution of the measurement is much longer than in a SAXS experiment. Reprinted with permission from ref. 57. Copyright 2011, American Chemical Society.

hydration levels of the micelles is observed for any of the different ions. In the connected study on the silica containing system[12] the authors observe that the presence of "salting-in" ions causes a larger polydispersity of the micelles already at the onset of the reaction, *i.e.* immediately following upon the addition of the silica source, and that this eventually leads to less well defined material in terms of the lattice parameter. Meanwhile the effect is the opposite when "salting-out" ions are present. The initial micellar state is thus reflected in the quality of the final material.

In an *in situ* SAXS investigation following the evolution of the hexagonal structure of SBA-15 synthesized with Pluronics P104 and simple sodium halide salts Teixeira *et al.*[22] observe disparities between the anions based on the Hofmeister series. The authors discuss that chloride provides a general ion effect resulting in dehydration of the corona region, while large polarizable anions, such as I^-, give rise to a counterbalancing specific ion effect. The general ion effect originates from decrease in solubility of the EO-segments as the polarity of the solvent is increased by the presence of ions in solvent media. Kabalnov *et al.*[63] explain this as an osmotic effect whereby a depletion of ions in the vicinity of the EO-segments causes a dehydration of the corona. The specific ion effect, which can, as mentioned above, act as a counterbalance to the general ion effect, is caused by large polarizable ions (such as I^-) adhering to the EO-segments, thus increasing their solubility. Teixeira *et al.*[22] argue that this affects not only the dimension of the micelles but also the dynamics of the system. The increased hydrophobic behaviour in the presence of chloride speeds up the dynamics and provides the means for formation of a material with improved order.

Organosilicates such as tetraethyl orthosilicate (TEOS) or tetramethyl orthosilicate (TMOS) are the most common sources of silica. Once they come into contact with water they will start

to hydrolyse into silicic acid and the corresponding alcohols. Under normal acidic conditions the silicic acid quickly starts to condense and polymerize, forming a silica network, rather than linear polymers.[64] It is well established that there is an attraction between silica and PEO, both through experimental and simulation work, and the hydrophobic effect has been suggested as its origin.[65–67]

In the acidic silica systems the hydrophobic effect has also been suggested as the driving force for association.[32] The coating of the Pluronic micelles by silica has been observed using both scattering[12,15,18,26,68] and spectroscopic[42] techniques. Khodakov *et al.*[15] as well as others[18,68] see an increase in intensity of the X-ray scattering attributed to micelles in solution after the addition of the silica source, which they interpret as an increase in electron density in the micelle corona–shell due to silica incorporation. Using EPR spectroscopy Ruthstein *et al.*[42] came to the same conclusion. There is a consensus regarding this aspect of the formation of SBA-15 and similar materials, and this is an essential step involved in propelling the formation forward towards the ordered solid material. As we shall see in the next section though results from various investigations point in slightly different directions and there are different opinions and interpretations separating the proposed mechanisms by which mesoporous silica, templated by non-ionic structure directors, form.

The micellar-to-structured material period

During the stage when the micellar solution evolves into liquid-like particles, and develops an internal structure, the system becomes more complicated to study. Processes occur at different length scales as well as time scales and there are both thermodynamic and kinetic effects to take into consideration. But this is also, in a sense, the most interesting period, as a thorough understanding of the progression opens up the possibility for a more effective and detailed tuning of the material properties, which is of key importance for designing materials. This section, as well as the following section on the particle development, is written in a chronological order, going from the early investigations to the very recent ones. We hope that this will provide a good overview on how the field has developed over the years.

We recall that there is a well-established association of silica with the highly hydrated PEO corona of the polymer micelles in solution and that silica condensation is fast under the acidic conditions most often used during synthesis. In an early *ex situ* SAXS study of the formation of SBA-15,[16] the authors followed the evolution of the unit-cell parameter by studying the (10) diffraction peak. The unit cell size is found to decrease with time after the initial appearance of the peak, for both normal SBA-15 as well as a large pore variant where 1,3,5-trimethylbenzene (TMB) had been added as a swelling agent to increase the core size of the polymer micelles. The formation of the hexagonal phase begins as soon as a white precipitate is formed and the authors discuss the relative intensity variations of the detected peaks. The evolution of both the unit cell size and the intensity of the (11) peak is explained to result from the on-going silica polymerization, silica being predominantly located between the micelles in the hexagonal structure. As the silica network grows denser, the structure is contracted and the electron density difference between the hydrophobic core and hydrophilic silica-containing corona is increased, thus leading to the higher peak intensity observed. In an EPR study in the same year, Ruthstein *et al.*[43] used spin-labelled Pluronic L62 (EO_6–PO_{30}–EO_6) to follow the formation process of SBA-15. The spin-labelled molecules partition at the core–corona interface, where they provide information on the changing environment of the probes as the synthesis proceeds. The results show a continuous depletion of water at this location. The authors also see a partitioning of the spin-probes between two different regions within the structure; in the eventual mesopores but also in the region of the walls, which after calcination becomes porous as well (*i.e.* intrawall pores). This intrawall porosity is a principal feature of SBA-15. The existence of intrawall pores was proposed to result from PEO segments penetrating the walls and thus connecting the ordered mesoporous channels.[9,10] Although the topic of this review is on events taking place during the synthesis, we will here still mention some interesting investigations done related to the intrawall porosity even though the studies are focused on events taking place after the initial 24 hours synthesis time at 35 °C. The connecting intrawall pores were found to increase in size from the micropore to the mesopore range when the hydrothermal treatment (note, called synthesis by the authors) of the material was done at 130 °C.[9] This was explained as a consequence of increased dehydration of the PEO-segments, which led to a phase separation of PEO from silica at "the nanometre scale, bringing about an increase in the size of the structural mesopores and a densification of the silica walls". In Fig. 6 a schematic representation of these changes in porosity with temperature is shown.

Following this, a number of publications appeared, focusing on investigating the mechanism by which the dilute micellar solution transformed into the ordered mesoporous material. Flodström *et al.* studied a system of P123 with TEOS or TMOS, respectively, as the silica source in two publications using different techniques.[18,32] In the first paper the system was studied using ^{1}H-NMR and TEM. Investigating the NMR peak of the methyl protons in the PO segments, a change occurs from a motionally narrowed signal, typically observed for spherical micelles in solution, to a broad one, indicative of a static system, around the same time as a white precipitate becomes visible to the unaided eye. The synthesis mixture was also studied by TEM (see the Techniques section) at different times before and after precipitation of material and found to go from aggregates (called flocs) of spherical micelles held together by silica to elongated micelles, which then align, eventually forming the hexagonal structure. The attraction between silica and EO is argued to originate from a hydrophobic effect and the on-going silica polymerization leads to bridging between silica covered micelles resulting in the subsequent liquid–liquid phase separation of a concentrated phase, a floc, in a dilute phase. Subsequently the micelles in the floc coalesce into cylinders that rearrange into the hexagonal phase. Emphasis is put on

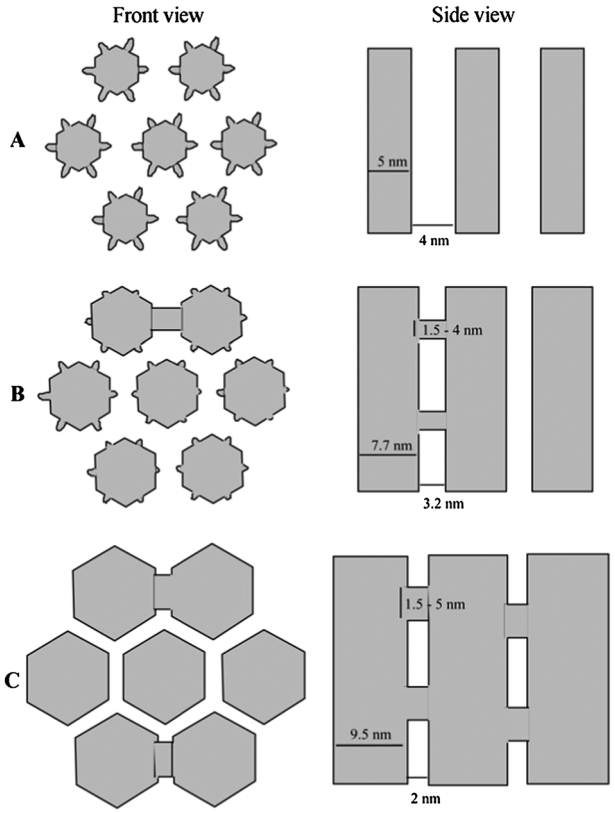

Fig. 6 The evolution of the porous structure of SBA-15 with increasing temperature, as envisioned in ref. 9. In this investigation the hydrothermal temperature, after an initial synthesis of 24 h at 35 °C, was varied. The porosity, both mesoporosity and intrawall porosity, was affected. The intrawall porosity was found to increase in size with temperature as a consequence of a phase separation of PEO from silica at ''the nanometer scale''. Reproduced from ref. 9 with permission from the Centre National de la Recherche Scientifique (CNRS) and The Royal Society of Chemistry.

the importance of hydrophobic attraction as the driving force in the formation of mesoporous materials from non-ionic structure directors. It is argued that hydrogen bonding between silica and ethylene oxide will provide little to no net driving force in aqueous solution. The second paper is an *in situ* SAXS investigation with modelling of the diffuse micellar scattering and analysis of the Bragg reflections. In the early stages (first 45 and 50 min in the case of TMOS and TEOS respectively) the recorded scattering data show only a single broad peak, indicative of spherical micelles. The micellar peak disappears simultaneously as the first Bragg reflection appears. The diffraction peak then continuously grows in intensity. The fact that precipitation is observed before the appearance of the Bragg reflections and their coexistence with the diffuse scattering of micelles is used as an argument in favour of the liquid–liquid phase separation of a concentrated phase of spherical micelles presented in the first investigation, *i.e.* the formation of flocs as mentioned above. It is also observed that even though the (10) peak continuously grows in intensity two of the higher order peaks actually decrease in intensity, due to relative contrast changes.[12,15]

More or less simultaneously Ruthstein *et al.*[42] published results from a new EPR-investigation on a system using H_3PO_4 as the acid, and hence a comparatively higher pH value during the synthesis. Several different spin probes were used to gather information from different regions (the core, the core/corona interface, the corona and the core/solvent interface) of the evolving system (see the schematic representation in Fig. 4). From the information gathered the authors describe a number of steps, starting with the penetration of hydrolysed TMOS and solvent, which was D_2O, into the micelle corona. From the experimental protocol the presence of deuterium in the vicinity of the spin-probe can be deduced. As time progresses, the signal intensity of D_2O/OD is reduced at the core/corona interface, and is explained as being caused by the increased silica polymerization in this region. The silica polymerization is then seen to continue but mainly in the corona region, leading to the conclusion that the polymerization starts in the micelle corona, close to the core, and then propagates outwards to the region between adjacent micelles. This is consistent with the changes seen in electron density profiles calculated from scattering curves in the previously mentioned *in situ* SAXS study.[18]

Results from an investigation looking at the effect of acidity, salt concentration and temperature on the evolution of particle morphologies were reported by Yu *et al.*[51] to describe what they call a ''colloidal phase separation mechanism''. The authors divide the mechanism into three stages, where the first one is a cooperative self-assembly process of silica and surfactants. Charge density matching is mentioned as being of importance. This is a concept initially used for the synthesis of ionic systems, suggested to proceed *via* interactions of the charged surfactant (S) and the charged inorganic (I) species, *e.g.* $(S^+)(I^-)$ or $(S^-)(I^+)$.[69] For the non-ionic synthesis, a mechanism mediated *via* hydrogen bonding to the polymer (S^0), the acid counter ion (X^-) and the positively charged silicate, *i.e.* $(S^0H^+)(X^-I^+)$ was suggested by Zhao *et al.*[5] This is followed by the second stage, called ''colloidal-like interactions'', that is described as further interaction and aggregation of the composite silica–surfactant moieties into larger colloidal objects with continued cross-linking of the silica, forming a new ''liquid crystal-like phase''. Following the liquid–liquid phase separation the reaction solution is seen to become turbid and shortly after, the authors observe spherical objects using SEM. The authors argue that during a phase separation the new phase will strive to minimize the surface free energy (F), and as a consequence spherical objects are formed, thus supporting the phase separation mechanism suggested. At this stage no ordered liquid crystal structure has yet been observed. The third stage is called a ''multiphase *energy competition*'' where the competition is between the free energy of mesophase formation (ΔG) and the surface free energy (F). We will return to this aspect later on in the section about the particle development.

In a later *in situ* SAXS study by Khodakov *et al.*[15] in 2005 focusing on the early stages of formation, the authors argue for a different system propagation than the one previously discussed.[18] Following the introduction of TEOS as the silica source a broad peak is observed in the scattering data from the silica–polymer micelles. The broad peak, it is argued, is more likely caused by the form factor of non-interacting objects

rather than short-distance correlation between objects, which would give a maximum in the structure factor term. The position of the peak is given as one of the reasons for this interpretation, as it is located at a larger scattering vector value *i.e.* shorter distance, than the unit cell parameter detected for the initial hexagonal structure formed later on. The scattering data are modelled to objects with cylindrical shape and the fits to the experimental data show good agreement even at low scattering angles. The experimental set-up used, identical to the one shown in Fig. 2, includes a 2D-detector, and anisotropy in the detected scattering is explained to be caused by alignment of cylindrical objects by the flow of the solution through the capillary used. The authors conclude that the collected data suggest that in the initial stages of synthesis, non-interacting cylindrical silica–polymer micelles are formed. Packing of the cylindrical micelles into larger domains with ordered hexagonal structure follows. A three-step electron density profile for the core, corona and surrounding environment is also modelled from the scattering data and is found to agree with previous investigations. As formation progresses, the density of the surrounding environment becomes more and more like the density of the corona, reflecting the increasing silica polymerization around the structure forming micelles.

The mechanism, relying on formation of elongated micelles that aggregate, was further supported in the first cryo-TEM study of SBA-15.[48] Images taken of the vitrified film of the initial reaction solution show only spheroidal micelles at the very early stages but eventually as the synthesis proceeds, threadlike micelles are detected (see Fig. 7), which are seen to grow larger and less flexible with time. The threadlike micelles are then observed to form bundles with sizes in the same range as what is observed for the final material. The use of cryo-TEM was limited to the first 40 min of synthesis due to the precipitation, after which freeze–fracture replication cryo-TEM was used instead. From freeze–fracture replication of the solution after 2 h 50 min of synthesis time the hexagonal structure is observed. The same order of events is seen for both a kinetically slower system, catalysed by H_3PO_4, as well as a faster system, using HCl as the acid. The results are discussed and interpreted together with previous EPR investigations[42,43] and it is suggested that a decrease in the curvature of the micelles due to the interaction with the polymerising silica is what drives the transformation from spheroidal to threadlike micelles. One earlier study[42] showed a decrease in the water content of the corona and the authors conclude that it is a consequence of the polymerisation of silica in the corona, which increases the hydrophobic character of the core–corona. The continuous change in polarity in the corona region was observed to continue long after precipitation was observed suggesting that it is rather the growth and aggregation of the threadlike micelles that cause the precipitation.

In the first *in situ* SANS study on the initial stages of SBA-15 formation Impéror-Clerc *et al.*[27] present results pointing in the same direction as the cryo-TEM[48] and *in situ* SAXS[15] discussed earlier. The reaction is carried out in deuterated solvent to provide good contrast between the organic micelles and the solvent, thereby making it possible to follow the reaction right from the onset of the synthesis. The scattering data are modelled as core–shell type spheres, ellipsoids or cylinders. During an initial induction period of about 5 min the scattering data are well described by spherical micelles after which a continuous change described by a transformation to cylindrical micelles is seen in the scattering pattern. The appearance of Bragg reflections, indicative of an ordered structure, is detected at the same time as the precipitation is observed. The authors conclude that this "proves that the precipitation phenomenon is associated with the self-assembly of hybrid cylindrical micelles into a two-dimensional hexagonal structure of SBA-15".

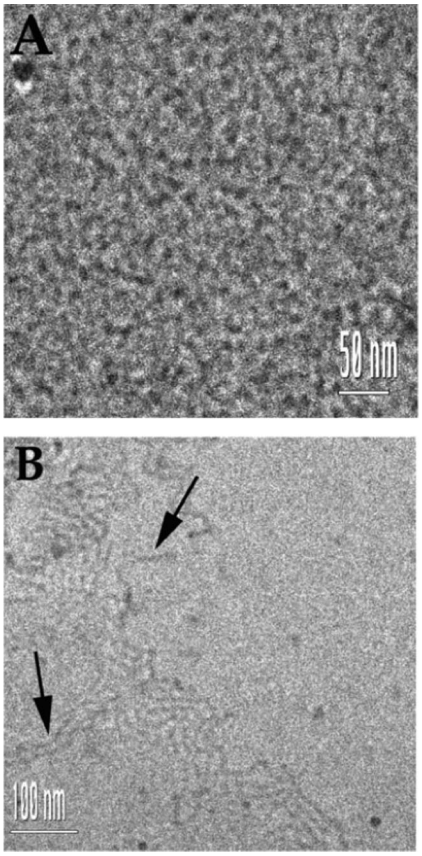

Fig. 7 Cryo TEM images of a reaction solution of SBA-15 taken from ref. 48. The images show in (A) spheroidal micelles and (B) threadlike micelles indicated by arrows. The spheroidal micelles are observed initially and after 22 minutes the micelles transformed into elongated micelles. Reprinted with permission from ref. 48. Copyright 2006, American Chemical Society.

At this point it can be useful to for a moment reflect upon the different interpretations of the propagation events for the systems under study. One set of studies argues for the formation of flocs of unordered spherical micelles, and that the micelles later elongate and evolve into a hexagonal structure. This happens after precipitation is observed. The other suggested pathway is the formation of elongated, silica decorated micelles, which later aggregate forming the hexagonal structure. As seen by several authors, changes in *e.g.* silica source,[13,18] acid,[12,29,48] co-solutes,[45,52] salt content[22] and stirring rate[37] can change kinetics, particle morphology and even the ordered structure of the material synthesized. Direct comparison between studies

performed under different synthesis conditions is therefore not without complications, and one should remain careful in drawing conclusions that are of a general nature.

An unexpected oriented aggregation behaviour of seven so-called ''primary particles'' during formation of plate-like SBA-15 particles synthesized by Pluronic P104 (EO_{27}–PO_{61}–EO_{27}) was observed by Linton and Alfredsson.[54] The system was further studied using *in situ* SAXS and USAXS to access length scales between 5–10 000 Å, thereby providing information on the aggregation of the large objects in addition to the information provided earlier in this review.[11] Four different synthesis temperatures were used and the resulting scattering curves from the *in situ* SAXS measurements were fitted to theoretical models. Initially the curves can be well modelled by a spherical core–shell model, but later on the curves change and cannot be modelled by either polydisperse spheres or cylinders. At the same time the appearance of larger objects in solution is detected by complementary UV-vis measurements. The scattering curves do, after another couple of minutes (time depending on the synthesis temperature), fit a polydisperse cylindrical model, meanwhile USAXS measurements show the presence of large objects. This illustrates a weakness of the scattering methodology being reliant on inexact models to interpret the data. The hexagonal phase takes some additional time before appearing, the diffraction peaks gradually increase in intensity while the intensity of the diffuse scattering from the micelles is continuously reduced. The results support the previously suggested mechanism by Flodström *et al.*[32] The micelles in the flocs eventually coalesce into cylindrical micelles and arrange in what is described as a ''nematic-like phase'', which later evolves into the hexagonal structure.

In a collaboration between a group in Gothenburg, Sweden, and one in Aarhus, Denmark, a new model for the analysis of *in situ* SAXS data was developed.[25] A factorization of the scattered intensity in one structure and one form factor contribution allows the same model to be used to follow the formation of mesoporous silica, from separate micelles and silica oligomers to the ordered structure. The model is applied to the investigation of a synthesis of SBA-15 at higher pH value (between 2 and 3) than what is typically used.[26] Due to the high pH the kinetics of the synthesis is slower allowing the formation to be followed in detail using a laboratory based SAXS instrument. An approach was used where the silica source, TEOS, was allowed to hydrolyse and condense for some time before mixing it with a Pluronic solution. The synthesis was followed *in situ* and analysed using the new SAXS model. From the results, complemented by DLS and TEM data, a mechanism is suggested. The attraction between silica and PEO, which is suggested to be of entropic origin and strongly dependent on the size of the silica oligomers, induces an elongation of the spherical micelles. As the polymerization continues, the attraction increases and aggregation and phase separation of silica–polymer particles follow. The particles will then go through internal rearrangement to eventually form a well-ordered hexagonal structure.

Further investigation of the formation process using Pluronic P104 as the structure director with different silica sources (TMOS, TEOS and TPOS) and different salts (NaCl and NaBr) was performed using *in situ* SANS.[13] In this study three different contrasts of the reagent solution were used, either with 100% D_2O, 100% H_2O or contrast matched to silica, respectively. SANS has the advantage over SAXS that by using different contrasts different chemical environments can be probed. The (10) Bragg peak was followed *in situ* and surprisingly found to decrease in intensity after its initial rapid appearance. This effect was clear when the solvent was 100% D_2O whereas in the silica matched solution the peak intensity was more or less constant. (The data from the 100% H_2O sample suffered from too high incoherent background to be properly analysed.) This is different from the behaviour observed in *in situ* SAXS studies following the same peak as mentioned above. The observation was attributed to the depletion of water from the siliceous layers surrounding the micelles in the ordered structure, which would decrease the difference in contrast between the ordered micelles and their surrounding environment when using D_2O as solvent. However using silica matched solution no difference would be observed. The observation further strengthens the view of an increasing density of the silica network encapsulating the organic micelles and is in agreement with earlier observations.[15,18,42] Effects on the unit-cell parameter and the dynamics of the reaction are also observed, and found to depend on the silica source, the salt content as well as the identity of the salt.

While the first SAXS and SANS studies performed focused mainly on systems containing only a Pluronic polymer, acid and a silica source, several papers were published during 2011 where the effect of different ions was explored. As mentioned earlier the presence of different salts can have a large effect on both pure polymer systems[57,62] as well as on the properties of mesostructured materials.[59,70,71]

Teixeira *et al.*,[22] as mentioned above, added different sodium halide salts to a synthesis based on Pluronic P104 and TEOS and studied the effects on phase separation (*i.e.* floc formation), mesophase formation and initial cell parameter by *in situ* SAXS measurements and visual observation. The results are in accordance with the anions being ordered in the Hofmeister series and the effects observed are discussed as originating from general and specific ion effects mentioned earlier (see The micellar period). Chloride is found to have the largest effect, caused by a general ion effect, with earlier onset of phase separation, mesophase formation and the largest initial cell parameter. It is followed in turn by bromide and iodide, where the general ion effect is counterbalanced by the specific ion effect.

As already mentioned, Manet *et al.* presented two comprehensive studies using both SAXS and SANS to investigate both the structure of Pluronic micelles in solution[57] and the formation of mesostructured silica *in situ*, *via* addition of TEOS to the micellar solution.[12] The authors use the advanced model previously mentioned[25] with several variable parameters to fit the scattering data. *In situ* Raman spectroscopy is also used to follow the hydrolysis of TEOS, and the hydrolysis is found to be complete within minutes ($\leq$10 min) after addition. A sphere-to-rod transition is observed after TEOS hydrolysis, suggested to be driven by the silica condensation. The value of a contrast

parameter called α (continuously increasing with time) is interpreted as an increase in the silica condensation in the micelle shell. The molar ratio of Si : EO in the shell just before precipitation is found to be close to that of the synthesis mixture, suggesting that most of the silica is found in the micelles at this point. The identity of the ions in solution is varied through use of different mineral acids, and ''salting-in'' ions give a high polydispersity (15–25%) of the micelles in solution (without siliceous species present) and the nucleating grains (with siliceous species present) are found to have several different distinct lattice spacings. The final materials prepared in the presence of ''salting-out'' ions have a higher homogeneity than those prepared with ''salting-in'' ions. The ''salting-in'' ions that specifically interact with the organic polymer are, qualitatively, said to compete or hinder the silica–polymer interaction, unlike the ''salting-out'' ions. A similar conclusion regarding the quality of the synthesized materials was drawn by Teixeira *et al.*,[22] their argument focusing on the faster dynamics observed in the presence of Cl^- (a ''salting-out'' ion) leading to a less cross-linked, more flexible silica structure at the time of mesophase formation. This would allow the structure to more effectively reach a thermodynamically stable state with straighter pores and more well defined ordering. They also detect fast disappearance of micellar scattering when salt is present, which is not unlike the faster nucleation in the presence of ''salting-out'' ions (compared to ''salting-in'' ions) observed by Manet *et al.* and that this gives more well defined properties. A possible explanation for differences observed in these two studies is that since Teixeira *et al.* use HCl as the acid, Cl^- is always present in the system.

In a very recent publication, Ruan *et al.*[49] use cryo-TEM to directly observe floc formation during synthesis of SBA-15 from Pluronic P104. Identical synthesis conditions as in the *in situ* SAXS/USAXS study by Linton *et al.*[11] were used. The flocs were observed early in the process and no internal order could be detected, consistent with the previous *in situ* SAXS study on the same system as no Bragg reflections had occurred at this point. The study also suggests a mechanism for control of the particle size (*i.e.* floc size) based on the transient colloidal stability (this is discussed further in the Particle development period).

So far the discussion has been centred on the formation of SBA-15, the hexagonally structured material. Several other structures synthesized with non-ionic surfactants exist as well, such as bicontinuous cubic KIT-6,[6] cubic SBA-16,[5] cubic FDU[8] and random wormhole structured MSU,[3] but the available literature on *in situ* studies on these materials is less comprehensive. For the remainder of this section these studies will be discussed.

As mentioned before, anions can have strong effects on the formation of mesoporous materials. Pluronic P103 (EO_{17}–PO_{59}–EO_{17}) for example can, in the presence of iodide, form a bicontinuous cubic structure (*Ia3d*).[70] The formation of this structure is compared with that of the micellar cubic (*Im3m*) SBA-16 structure synthesized with Pluronic F108 (EO_{132}–PO_{50}–EO_{132}) using *in situ* SAXS and NMR.[19] For the micellar cubic structure the authors see a similar progression with floc formation as observed for SBA-15.[18,32] Throughout the entire synthesis, also after the formation of the ordered structure, the authors register a broad peak from the scattering contributions of disordered micelles. The formation of the bicontinuous structure however is different from both the formation of SBA-15 and of SBA-16. Already before the addition of the silica source, the system has phase separated into a concentrated phase dispersed as small droplets (due to stirring) in a dilute phase. No micellar scattering is detected, but neither is any ordered structure, so the polymer is suggested to exist as a disordered bicontinuous concentrated phase. It is argued that the concentrated phase acts as an already preassembled structure director from the start, and as silica enters this phase the structure is rapidly formed. The Bragg peaks are visible after only 10 minutes. The authors picture this formation as a ''micro true liquid crystal templating mechanism''. Both systems are also studied with ^{1}H-NMR, following the protons on the methyl-groups of the PPO. For SBA-16, a single peak is detected and with time a broadening is observed. Two possible explanations are given, the first one being that a distortion of the micellar shape would lead to the observed broadening, the other that the motion of the polymer chain is restricted due to the EO-chains becoming trapped in the polymerising silica network. For the bicontinuous cubic system two peaks are observed, one from polymers in the concentrated phase and one from polymers in the dilute phase. A slight narrowing of the peak corresponding to the concentrated phase is observed, explained by the formation of more uniform domains. Comparing the results from the two NMR experiments, the authors argue that since line narrowing is observed for the bicontinuous system, the broadening observed for the micellar cubic SBA-16 and hexagonal SBA-15 is not caused by immobilization of the hydrophilic polymer segments within the silica matrix, as it is not observed in the bicontinuous system.

The bicontinuous cubic material KIT-6, reported by Kleitz *et al.* in 2003,[6] utilises butanol to change the phase behaviour of Pluronic P123. It is seen that insufficient amount of butanol leads to the normal hexagonal structure of SBA-15. However, with enough butanol it is observed, using low angle XRD, that structures with lower curvature are formed, first a lamellar structure and then later the bicontinuous cubic one. The formation of KIT-6 was studied further in two papers from the Israeli group of Daniella Goldfarb.[44,45] In one of the papers the evolution of the hydrophobic core of the structure forming micelles is studied using EPR and a spin-probe localized inside the micellar core. In the early stages of synthesis, swelling of the core is observed, together with a small decrease in aggregation number. The authors attribute this to the incorporation of TEOS in the core. Later on the micelles again return to their original size range.[44] In the second paper[45] several different spin probes are used to gather information from different parts of the evolving system by use of different EPR-techniques, much like the investigation of the formation of SBA-15 discussed earlier.[42] Based on the results of this investigation, which also included cryo-TEM imaging and freeze–fracture replication, a five stage process is presented. The first step is the by now familiar condensation of silica at the micelle/solvent interface

which is followed by the second step, a depletion of water and butanol from the core/corona interface. The third step is a transformation of spheroidal to threadlike micelles, which occurs at around the time as precipitation is observed. The fourth step, accelerated condensation of silica in the micelle corona and increased depletion of water and butanol from the core/corona, is detected as the aggregated threadlike micelles form a hexagonal structure. The hexagonal structure is then, in the fifth step, transformed to the bicontinuous cubic one, a step that is the focus of another study discussed below.[52] The role of butanol in the formation of the cubic phase is discussed based on the results. During the fourth stage when the hexagonal phase is formed, butanol is displaced from the core/corona interface to the more hydrophilic corona/water interface. The authors suggest that once there, butanol will lower the surface curvature leading to the formation of the cubic structure. They also show that addition of butanol to a normal SBA-15 synthesis, after the formation of the hexagonal structure but before extensive cross-linking of the silica network, leads to a bicontinuous cubic structure. The bicontinuous cubic structure was previously suggested to form *via* a lamellar intermediate phase[6] although in the latter case the samples had dried prior to the X-ray analysis. The common denominator for these two results is that the formation proceeds *via* an intermediate structure. As mentioned earlier the transformation from hexagonal to bicontinuous cubic structure was the topic of a comprehensive investigation, using cryo-SEM and freeze–fracture replication TEM.[52] Two mechanisms are suggested, where in the major one the cylinders of the hexagonal phase merge together, forming a so-called perforated lamellar phase, which then in turn forms the bicontinuous cubic phase. A minor mechanism, the direct formation of the bicontinuous cubic phase from the hexagonal phase *via* so-called cylinder branching, is also presented. These observations are in accordance with the ones made by Kleitz *et al.*[6] and with the EPR and cryo-TEM study by Ruthstein *et al.*[45]

The particle development period

In this section the focus will be on investigations into the particle morphology, size and aggregation behaviour. The processes discussed in the previous sections affect these aspects as well, but due to the liquid-like nature of the materials during the earlier stages of formation, it is difficult to investigate these material properties. Morphology is best viewed through direct observation techniques, *e.g.* electron microscopy, which requires a certain degree of silica connectivity to be applicable. While there is a huge amount of literature showing the possibility to obtain different morphologies and particle sizes, the focus has rarely been to describe how the particles/morphologies are established.

In the seminal SBA-15 paper, SEM images of the as synthesized material are described as having "many rope-like domains with relatively uniform sizes of ~1 μm, which are aggregated into wheat-like macrostructures".[4] This type of elongated structure, often fibre-like in appearance, is indeed the most common manifestation of SBA-15. Considering the hexagonal packing of long cylinders forming the structure, this is perhaps not so unexpected. In an early paper, the addition of co-solvents, co-surfactants and inorganic electrolytes as well as the variation of the silica source resulted in a number of different morphologies.[72] For example, using TMOS as the silica source results in fibres made up of bundles of wires, sometimes hundreds of microns long. If TEOS is used under the same conditions shorter rope-like particles form instead. It is argued that the local curvature energy at the silica–block copolymer interface is of great importance for the particle morphology of SBA-15.

Based on their proposed "Colloidal phase separation mechanism" (see above), Yu *et al.*[51] discuss how different synthesis conditions affect the morphology of the developing particles. They have studied the formation of particles using SEM, both by looking at the final material and also by investigating the material at certain times after the precipitation. As we previously have touched upon their proposed mechanism is based on a competition between the surface free energy (F) and the free energy of mesophase formation (ΔG). The rate of formation is said to be of importance and a slow formation is in favour of morphologies with large curvatures, as the surface free energy will have a large influence. If the formation is rapid the particles will instead tend towards more crystal-like morphologies, such as hexagonal platelike for hexagonal structure or rhombdodecahedrons for cubic ($Im3m$) structure. Hence the authors conclude that conditions that favour slower formation, *e.g.* low acidity, low temperature and low ionic strength, lead to structures with higher curvature and minimized surface areas.

In a series of papers Linton *et al.* investigate the aggregation behaviour of a SBA-15 system based on Pluronic P104.[11,54–56] The first paper shows how hexagonal plate-like particles (called secondary particles) are built up from seven smaller entities (referred to as primary particles) that undergo an oriented aggregation step (shown schematically in Fig. 8). The formation is suggested to transpire *via* four steps, where the later two relate to particle formation. In a very recent paper by Ruan *et al.*[49] this theory was expanded and will be discussed in more detail below. In an attempt to gather more information about the oriented aggregation step Linton *et al.* performed the combined SAXS and USAXS study, that we have mentioned

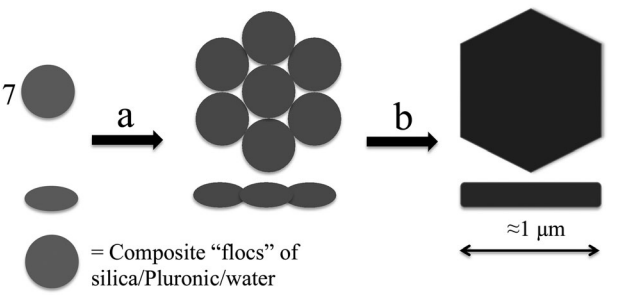

Fig. 8 A schematic representation (top and side view) of the oriented aggregation step whereby seven primary particles aggregate (along a direction perpendicular to 001) to form a secondary particle (a) that then develops a hexagonal platelike morphology through fusing and rearrangement (b). The final particle is essentially a single crystal but frequently defects (see ToC) are visible resulting from the aggregation behaviour. Adapted with permission from ref. 49. Copyright 2012 American Chemical Society.

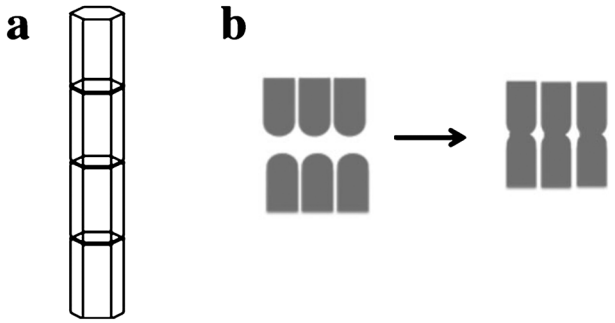

Fig. 9 Schematic representation of (a) oriented aggregation of primary particles along the (001) faces to form a fibre structure and (b) cylindrical micelles release strain induced by the higher curvature at the endcaps of the (001) faces *via* association with another (001) face. Reproduced from ref. 56 with permission from the PCCP Owner Societies.

earlier, but were unsuccessful in catching that particular step in the USAXS measurements, even though a well detailed timeline of events was established through use of several experimental techniques (see Fig. 1).[11] The authors had found that depending on the synthesis temperature, the particles formed were either hexagonal platelike (composed of seven primary particles) at 50 and 55 °C, primary particles (slightly elongated) at 60 °C, elongated primary particles at 65 °C and primary particles aggregated into fibres at higher temperatures. The latter type of morphology is very similar to what is often observed for SBA-15, suggesting that it is a rather general behaviour. A model is presented which describes the results based on differences in the behaviour of the Pluronic micelles and surface energies.[56] At lower temperature, aggregation at the faces perpendicular to the (001) face is favoured. As the temperature increases it is suggested that a strain is induced in the end caps of the cylindrical micelles at the (001) face. Eventually the micelles will try to release the strain by associating with another (001) face, thus forming the fibre structure. This is shown schematically in Fig. 9. Based on this and on the timeline established previously,[11] the effect of salt on the oriented aggregation behaviour shown in Fig. 8 was investigated. Addition at the onset of the oriented aggregation is found to increase this oriented aggregation, resulting in large platelike particles, up to 5 μm across, meanwhile the thickness of the particles remains unaffected. The system contains 1.6 M HCl, yet an addition of only 0.01 M NaCl is still found to have a noticeable effect. It is also observed that the effect of NaI is larger than that of NaCl, suggesting yet again that ion-specific effects are very important in Pluronic based syntheses. If the salt was added to the synthesis already from the start, *i.e.* before the addition of the silica source, the results were very different, demonstrating the possibility to achieve different results by introducing changes to the conditions as the system progresses. This approach has been used successfully to almost completely remove the intrawall porosity of SBA-15 by simple addition of 1 M NaI at an appropriate time.[71] Similarly, Chen *et al.* synthesised functionalized hexagonal platelike particles of SBA-15 from Pluronic P123 by addition of organosilanes 1–4 h after addition of TEOS.[59] The same group also showed that the time of addition of TMB to achieve pore swelling is of importance.[58] When TMB was added before the silica source, neither structure nor morphology of the material was well-defined. Addition 25–30 minutes after the onset of synthesis resulted on the other hand in a well-defined structure, larger pores and with the desired hexagonal platelike morphology maintained. Further delaying the addition gave the desired morphology and a good structure, but without swelling of the pores. This is consistent with the results of Reichhardt *et al.*[71] where an optimum time of addition was observed as well. Evidently it is possible to influence the internal structure when the development of the size and morphology is largely complete. The system used in previous studies[54,56] was investigated with cryo-TEM and high resolution SEM by Ruan *et al.*[49] and it was observed that particles with hexagonal platelike morphology could be observed by HRSEM (by freeze–drying of the reaction solution) already 29 minutes after addition of the silica source. From the results of the study the authors suggest a mechanism governing the size of particles. Pluronic molecules, possibly in concert with short silica oligomers, located at the floc/solution interface, and referred to as ''brushes'', provide colloidal stabilisation by steric means. As the flocs grow, the coverage of stabilising molecules increases until a stable size is reached (determined by the area/volume ratio). Eventually though the stabilising brushes are restricted by the increasing degree of silica connectivity and the stability is lost leading to aggregation of particles.

A systematic study of particle morphology and size, depending on several parameters, was recently published.[37] At low synthesis temperature the particles take on a spherical morphology (with poor mesoscopic ordering) but at increasingly higher synthesis temperatures hexagonal platelike particles, followed by so-called ''rice-shaped'' particles, rods and finally donut-shaped are obtained. The ''rice-shaped'' particles are very similar to the elongated primary particles observed by Linton *et al.*[56] and thus it seems that the evolution of particle morphologies is the same. This is not consistent with the ''Colloidal phase separation mechanism'' reported by Yu *et al.*[51] that propose the formation of particles with higher curvature when the temperature is lowered. However, Lee *et al.* used different, rather high stirring rates during their synthesis and observed an effect from that, while Yu *et al.* synthesized the particles under static conditions.

Conclusions

Although much progress has been made in elucidating the mechanism by which these materials form one has still not arrived at a unified comprehensive description of the molecular events. Different studies may point in different directions, but also present many similarities, suggesting that there may exist several paths to reach the final material. The rich phase behaviour of the Pluronic molecules used as structure directors plays a crucial role during synthesis and tuning their behaviour can change material properties from the meso- to the micro-scale. Different additives in the synthesis solution and varying the reaction temperature are both complications as well as sources of great potential, especially when considering that different

material properties can be targeted at different times (during the formation) when the progression of the system is understood.

These points highlight the need for a solid understanding of formation mechanisms, both for practical and academic reasons. In this tutorial review we have compiled the relevant results from a range of studies aimed at elucidating the formation events of materials formed with non-ionic structure directors, in particular SBA-15. It is clear that probing different length scales, particularly using *in situ* measurements, is required to provide a comprehensive understanding, and that both thermodynamic and kinetic factors are fundamental.

References

1 J. S. Beck, J. C. Vartuli, W. J. Roth, M. E. Leonowicz, C. T. Kresge, K. D. Schmitt, C. T. W. Chu, D. H. Olson and E. W. Sheppard, *J. Am. Chem. Soc.*, 1992, **114**, 10834–10843.
2 S. Inagaki, Y. Fukushima and K. Kuroda, *J. Chem. Soc. Chem. Commun.*, 1993, 680–682.
3 S. A. Bagshaw, E. Prouzet and T. J. Pinnavaia, *Science*, 1995, **269**, 1242–1244.
4 D. Zhao, J. Feng, Q. Huo, N. Melosh, G. H. Fredrickson, B. F. Chmelka and G. D. Stucky, *Science*, 1998, **279**, 548.
5 D. Zhao, Q. Huo, J. Feng, B. F. Chmelka and G. D. Stucky, *J. Am. Chem. Soc.*, 1998, **120**, 6024–6036.
6 F. Kleitz, S. Hei Choi and R. Ryoo, *Chem. Commun.*, 2003, 2136–2137.
7 S. Che, A. E. Garcia-Bennett, T. Yokoi, K. Sakamoto, H. Kunieda, O. Terasaki and T. Tatsumi, *Nat. Mater.*, 2003, **2**, 801–805.
8 C. Yu, Y. Yu and D. Zhao, *Chem. Commun.*, 2000, 575–576.
9 A. Galarneau, H. Cambon, F. Di Renzo, R. Ryoo, M. Choi and F. Fajula, *New J. Chem.*, 2003, **27**, 73–79.
10 R. Ryoo, C. H. Ko, M. Kruk, V. Antochshuk and M. Jaroniec, *J. Phys. Chem. B*, 2000, **104**, 11465–11471.
11 P. Linton, A. R. Rennie, M. Zackrisson and V. Alfredsson, *Langmuir*, 2009, **25**, 4685–4691.
12 S. Manet, J. Schmitt, M. Impéror-Clerc, V. Zholobenko, D. Durand, C. L. P. Oliveira, J. S. Pedersen, C. Gervais, N. Baccile, F. Babonneau, I. Grillo, F. Meneau and C. Rochas, *J. Phys. Chem. B*, 2011, **115**, 11330–11344.
13 P. Linton, A. R. Rennie and V. Alfredsson, *Solid State Sci.*, 2011, **13**, 793–799.
14 F. Michaux, J.-L. Blin, J. Teixeira and M. J. Stébé, *J. Phys. Chem. B*, 2011, **116**, 261–268.
15 A. Y. Khodakov, V. L. Zholobenko, M. Impéror-Clerc and D. Durand, *J. Phys. Chem. B*, 2005, **109**, 22780–22790.
16 V. L. Zholobenko, A. Y. Khodakov and D. Durand, *Microporous Mesoporous Mater.*, 2003, **66**, 297–302.
17 R. Atluri, N. Hedin and A. E. Garcia-Bennett, *Chem. Mater.*, 2008, **20**, 3857–3866.
18 K. Flodström, C. V. Teixeira, H. Amenitsch, V. Alfredsson and M. Lindén, *Langmuir*, 2004, **20**, 4885–4891.
19 K. Flodström, H. Wennerström, C. V. Teixeira, H. Amenitsch, M. Lindén and V. Alfredsson, *Langmuir*, 2004, **20**, 10311–10316.
20 J. Morell, C. V. Teixeira, M. Cornelius, V. Rebbin, M. Tiemann, H. Amenitsch, M. Fröba and M. Lindén, *Chem. Mater.*, 2004, **16**, 5564–5566.
21 M. Lindén, S. A. Schunk and F. Schüth, *Angew. Chem., Int. Ed.*, 1998, **37**, 821–823.
22 C. V. Teixeira, H. Amenitsch, P. Linton, M. Lindén and V. Alfredsson, *Langmuir*, 2011, **27**, 7121–7131.
23 A. Lind, J. Andersson, S. Karlsson, P. Ågren, P. Bussian, H. Amenitsch and M. Lindén, *Langmuir*, 2002, **18**, 1380–1385.
24 T. Nakamura, M. Mizutani, H. Nozaki, N. Suzuki and K. Yano, *J. Phys. Chem. C*, 2006, **111**, 1093–1100.
25 A. Sundblom, C. L. P. Oliveira, A. E. C. Palmqvist and J. S. Pedersen, *J Phys. Chem. C*, 2009, **113**, 7706–7713.
26 A. Sundblom, C. L. P. Oliveira, J. S. Pedersen and A. E. C. Palmqvist, *J. Phys. Chem. C*, 2010, **114**, 3483–3492.
27 M. Impéror-Clerc, I. Grillo, A. Y. Khodakov, D. Durand and V. L. Zholobenko, *Chem. Commun.*, 2007, 834–836.
28 M. J. Hollamby, D. Borisova, P. Brown, J. Eastoe, I. Grillo and D. Shchukin, *Langmuir*, 2011, **28**, 4425–4433.
29 A. Berggren and A. E. C. Palmqvist, *J. Phys. Chem. C*, 2008, **112**, 732–737.
30 M. Mesa, L. Sierra and J.-L. Guth, *Microporous Mesoporous Mater.*, 2008, **112**, 338–350.
31 S. C. Christiansen, D. Zhao, M. T. Janicke, C. C. Landry, G. D. Stucky and B. F. Chmelka, *J. Am. Chem. Soc.*, 2001, **123**, 4519–4529.
32 K. Flodström, H. Wennerström and V. Alfredsson, *Langmuir*, 2003, **20**, 680–688.
33 N. A. Melosh, P. Lipic, F. S. Bates, F. Wudl, G. D. Stucky, G. H. Fredrickson and B. F. Chmelka, *Macromolecules*, 1999, **32**, 4332–4342.
34 C. C. Egger, M. W. Anderson, G. J. T. Tiddy and J. L. Casci, *Phys. Chem. Chem. Phys.*, 2005, **7**, 1845–1855.
35 D. Margolese, J. A. Melero, S. C. Christiansen, B. F. Chmelka and G. D. Stucky, *Chem. Mater.*, 2000, **12**, 2448–2459.
36 N. Hedin, R. Graf, S. C. Christiansen, C. Gervais, R. C. Hayward, J. Eckert and B. F. Chmelka, *J. Am. Chem. Soc.*, 2004, **126**, 9425–9432.
37 H. I. Lee, J. H. Kim, G. D. Stucky, Y. Shi, C. Pak and J. M. Kim, *J. Mater. Chem.*, 2010, **20**, 8483–8487.
38 D. Baute, V. Frydman, H. Zimmermann, S. Kababya and D. Goldfarb, *J. Phys. Chem. B*, 2005, **109**, 7807–7816.
39 A. Galarneau, F. D. Renzo, F. Fajula, L. Mollo, B. Fubini and M. F. Ottaviani, *J. Colloid Interface Sci.*, 1998, **201**, 105–117.
40 J. Zhang, Z. Luz and D. Goldfarb, *J. Phys. Chem. B*, 1997, **101**, 7087–7094.
41 J. Zhang, Z. Luz, H. Zimmermann and D. Goldfarb, *J. Phys. Chem. B*, 1999, **104**, 279–285.
42 S. Ruthstein, V. Frydman and D. Goldfarb, *J. Phys. Chem. B*, 2004, **108**, 9016–9022.
43 S. Ruthstein, V. Frydman, S. Kababya, M. Landau and D. Goldfarb, *J. Phys. Chem. B*, 2003, **107**, 1739–1748.
44 S. Ruthstein and D. Goldfarb, *J. Phys. Chem. C*, 2008, **112**, 7102–7109.

45 S. Ruthstein, J. Schmidt, E. Kesselman, R. Popovitz-Biro, L. Omer, V. Frydman, Y. Talmon and D. Goldfarb, *Chem. Mater.*, 2008, **20**, 2779–2792.
46 S. Sadasivan, C. E. Fowler, D. Khushalani and S. Mann, *Angew. Chem., Int. Ed.*, 2002, **41**, 2151–2153.
47 O. Regev, *Langmuir*, 1996, **12**, 4940–4944.
48 S. Ruthstein, J. Schmidt, E. Kesselman, Y. Talmon and D. Goldfarb, *J. Am. Chem. Soc.*, 2006, **128**, 3366–3374.
49 J. Ruan, T. Kjellman, Y. Sakamoto and V. Alfredsson, *Langmuir*, 2012, **28**, 11567–11574.
50 R. Che, D. Gu, L. Shi and D. Zhao, *J. Mater. Chem.*, 2011, **21**, 17371–17381.
51 C. Yu, J. Fan, B. Tian and D. Zhao, *Chem. Mater.*, 2004, **16**, 889–898.
52 L. Omer, S. Ruthstein, D. Goldfarb and Y. Talmon, *J. Am. Chem. Soc.*, 2009, **131**, 12466–12473.
53 S. M. Stevens, K. Jansson, X. Changhong, S. Asahina, M. Lingstedt, D. Grüner, Y. Sakamoto, K. Miyasaka, P. Cubillas, R. Brent, L. Han, S. Che, R. Ryoo, D. Zhao, M. Anderson, F. Schüth and O. Terasaki, *JEOL News*, 2009, **44**, 17–22.
54 P. Linton and V. Alfredsson, *Chem. Mater.*, 2008, **20**, 2878–2880.
55 P. Linton, H. Wennerström and V. Alfredsson, *Phys. Chem. Chem. Phys.*, 2010, **12**, 3852–3858.
56 P. Linton, J.-C. Hernandez-Garrido, P. A. Midgley, H. Wennerstrom and V. Alfredsson, *Phys. Chem. Chem. Phys.*, 2009, **11**, 10973–10982.
57 S. Manet, A. Lecchi, M. Impéror-Clerc, V. Zholobenko, D. Durand, C. L. P. Oliveira, J. S. Pedersen, I. Grillo, F. Meneau and C. Rochas, *J. Phys. Chem. B*, 2011, **115**, 11318–11329.
58 S.-Y. Chen, Y.-T. Chen, J.-J. Lee and S. Cheng, *J. Mater. Chem.*, 2011, **21**, 5693–5703.
59 S.-Y. Chen, C.-Y. Tang, W.-T. Chuang, J.-J. Lee, Y.-L. Tsai, J. C. C. Chan, C.-Y. Lin, Y.-C. Liu and S. Cheng, *Chem. Mater.*, 2008, **20**, 3906–3916.
60 G. Karlstroem, *J. Phys. Chem.*, 1985, **89**, 4962–4964.
61 P. Alexandridis and T. Alan Hatton, *Colloids Surf., A*, 1995, **96**, 1–46.
62 P. Alexandridis and J. F. Holzwarth, *Langmuir*, 1997, **13**, 6074–6082.
63 A. Kabalnov, U. Olsson and H. Wennerström, *J. Phys. Chem.*, 1995, **99**, 6220–6230.
64 H. E. Bergna, *Colloidal Silica Fundamentals and Applications*, CRC Press, Taylor & Francis Group, Boca Raton, FL, 2006.
65 M. Malmsten, P. Linse and T. Cosgrove, *Macromolecules*, 1992, **25**, 2474–2481.
66 L. M. Grant, F. Tiberg and W. A. Ducker, *J. Phys. Chem. B*, 1998, **102**, 4288–4294.
67 G. J. Howard and P. McConnell, *J. Phys. Chem.*, 1967, **71**, 2974–2981.
68 C. Boissière, A. Larbot, C. Bourgaux, E. Prouzet and C. A. Bunton, *Chem. Mater.*, 2001, **13**, 3580–3586.
69 Q. Huo, D. I. Margolese, U. Ciesla, P. Feng, T. E. Gier, P. Sieger, R. Leon, P. M. Petroff, F. Schuth and G. D. Stucky, *Nature*, 1994, **368**, 317–321.
70 K. Flodström, V. Alfredsson and N. Källrot, *J. Am. Chem. Soc.*, 2003, **125**, 4402–4403.
71 N. Reichhardt, T. Kjellman, M. Sakeye, F. Paulsen, J.-H. Smatt, M. Linden and V. Alfredsson, *Chem. Mater.*, 2011, **23**, 3400–3403.
72 D. Zhao, J. Sun, Q. Li and G. D. Stucky, *Chem. Mater.*, 2000, **12**, 275–279.